THE POTENTIAL FOR AMBIENT PLASMA WAVE PROPULSION

James H. Gilland, George J. Williams

Ohio Aerospace Institute

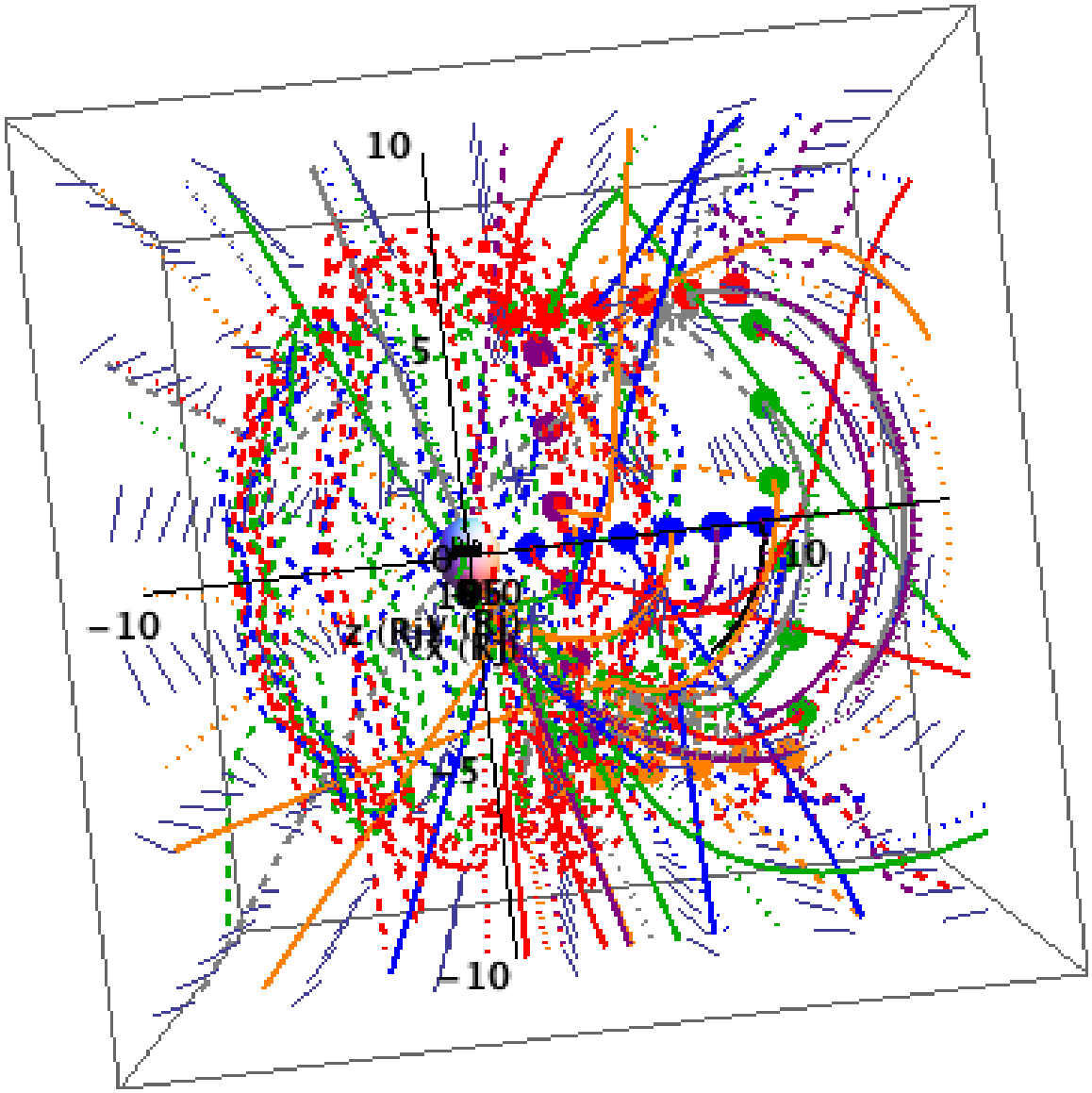

THE POTENTIAL FOR AMBIENT PLASMA WAVE PROPULSION

James H. Gilland, George J. Williams

Ohio Aerospace Institute
22800 Cedar Point Rd. Brook Park, OH 44142
jamesgilland@oai.org

I.Introduction

A truly robust space exploration program will need to make use of in-situ resources as much as possible to make the endeavor affordable. Most space propulsion concepts are saddled with one fundamental burden; the propellant needed to produce momentum. The most advanced propulsion systems currently in use utilize electric and/or magnetic fields to accelerate ionized propellant. However, significant planetary exploration missions in the coming decades, such as the now canceled Jupiter Icy Moons Orbiter[1], are restricted by propellant mass and propulsion system lifetimes, using even the most optimistic projections of performance. These electric propulsion vehicles are inherently limited in flexibility at their final destination, due to propulsion system wear, propellant requirements, and the relatively low acceleration of the vehicle.

A few concepts are able to utilize the environment around them to produce thrust: Solar[2] or magnetic sails[3] ,[4] and, with certain restrictions, electrodynamic tethers[5] . These concepts focus primarily on using the solar wind or ambient magnetic fields to generate thrust. Technically immature, quasi-propellantless alternatives lack either the sensitivity or the power to provide significant maneuvering[6]. An additional resource to be considered is the ambient plasma and magnetic fields in solar and planetary magnetospheres. These environments, such as those around the Sun or Jupiter, have been shown to host a variety of plasma waves.

Plasma wave propulsion takes advantage of an observed astrophysical and terrestrial phenomenon: Alfven waves. These are waves that propagate in the plasma and magnetic fields around and between planets and stars. The generation of Alfven waves in ambient magnetic and plasma fields to generate thrust is proposed as a truly propellantless propulsion system which may enable an entirely new matrix of exploration missions.

Alfven waves are well known, transverse electromagnetic waves that propagate in magnetized plasmas at frequencies below the ion cyclotron frequency. They have been observed in both laboratory and astrophysical settings[7],[8]. On Earth, they are being investigated as a possible means for plasma heating, current drive, and momentum addition in magnetic confinement fusion systems[9]. In addition, Alfven waves have been proposed as a mechanism for acceleration of the solar wind away from the sun[10].

A. Concept Description

In order to couple to the ambient plasma and magnetic environment, an Alfven wave propulsion system requires a properly designed antenna and AC power at the proper frequency to launch Alfven waves (Figure 1). The antenna design and frequencies will be determined by the plasma environment and the Alfven wave dispersion relation. Antenna scales will be on the order of a

wavelength, and frequencies will be below the ion cyclotron frequency of the environment. Under these conditions, the concept works by directionally generating Alfven waves along the ambient magnetic field, resulting in radiation pressure that produces thrust on the antenna.

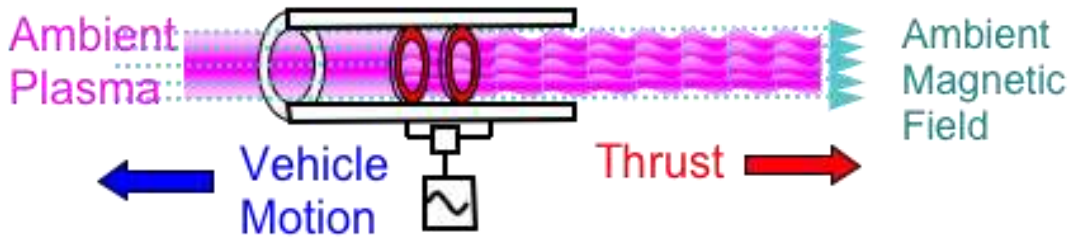

Figure 1. Schematic of plasma wave propulsion system. RF energy is coupled into the plasma generating Alfven waves which travel along the ambient magnetic field.

The generated thrust is proportional to the perturbed magnetic field strength in the waves, δB^2, and the area of the antenna. In order to launch linear Alfven waves, the perturbation must be less than the ambient field, which imparts a limit on the thrust density of this concept, unless non-linear effects are to be incorporated and considered. The parameters of operation for this concept in several representative environments are examined in a later section to determine the initial scaling needed.

B. Analysis Objectives

This research has been aimed at establishing the feasibility of launching human-generated Alfven waves in a planetary magnetosphere, and to examine the corresponding system parameters, scaling, and power levels required. This has focused on two areas: Assessing the wave propagation in relevant environments and examining the coupling of an antenna system to the environment in terms of power and efficiency.

1. *Wave Propagation Analysis*

Wave propagation was examined using the ray tracing method, which follows the wave group velocity (energy flow) as it moves through a spatially varying environment[11]. This was modeled using the cold plasma dispersion relation for the Alfven wave, which includes several modes of propagation (described in Section II) at differing angles to the magnetic field. The modeling was derived from first principles using Mathematica to progress from conservation equations to the numerical integration of the dispersion through magnetospheric environments, which were input into the code as axis-symmetric functions of {r, z} for Jupiter and the Earth.

The dispersion relation was derived for three dimensional magnetic and plasma density fields; however, with the exception of the magnetotails, and some effects from solar wind pressure, the majority of the fields were spherically symmetric. Magnetospheres were modeled as dipoles using experimental data and past models, and plasma density radial profiles were taken from planetary data.

The analysis was performed by calculating the axial wave numbers (k_z) for the various Alfven modes for the overall environment. A nominal frequency of 0.2 the local ion cyclotron frequency

(Ω_{ci}) was used. These values were used as the initial conditions for launching Alfven waves over a range of radial and axial positions, and examining their directions. Of interest was whether the waves would reflect and return to the launching site, which would negate their propulsive benefit as it would establish a standing wave with no group velocity.

2. Wave Launching System Analysis

To analyze the coupling of a real antenna to the ambient plasma, a launching code developed for cylindrical fusion systems, such as tandem mirrors, was used. The code used was the ANTENA code[12]. ANTENA is a 2 species (ion and electron) numerical code that models antenna spectra and their coupling to possible modes in a cylindrical, axially uniform plasma and magnetic field with user specified radial density profiles. The code was originally developed to calculate wave fields and plasma heating in the ion cyclotron range of waves; this regime includes the Alfven waves considered here.

ANTENA was not intended as a space simulation code, so some adaptations have to be made. The reference ANTENA geometry is shown in Figure 2. In this geometry, the antenna is assumed to be outside of the plasma. In an aerospace context, this will not necessarily be the case; however, this model approximates a best case antenna coupling situation to assess the concept's feasibility.

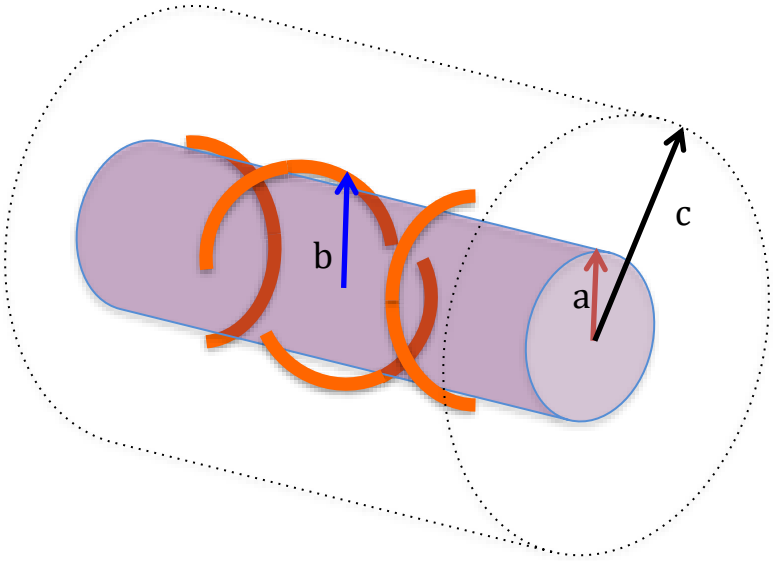

Figure 2. ANTENA plasma –antenna geometry: a= plasma radius, b= antenna radius, c=ground plane radius.

The antenna arrangement shown, of phased half loops, was chosen to assess the effects of antenna spacing on overall plasma coupling. The antenna was modeled with the straps fed in parallel, with different phasings of current between the straps. It does not represent an optimized configuration, but allows for assessment of the antenna coupling issues for this concept.

II.Background

Several physical issues determine the feasibility of ambient wave propulsion: the characteristics of the waves, the environmental conditions, and the overall system scales and efficiencies in generating waves in the plasma. The important relations that must be examined are described here.

A. Plasma Waves

Plasma waves are propagated through the acoustic or electromagnetic perturbation of ions and electrons relative to the ambient magnetic field. The type of wave generated depends on the frequency of the perturbation relative to the natural frequencies of the plasma, such as the ion and electron cyclotron frequencies, and the plasma frequencies:

$$\begin{aligned} W_{ci} &= \frac{qB}{M_i} \\ W_{ce} &= \frac{qB}{m_e} \\ w_{pi} &= \frac{nq^2}{e_0 M_i} \\ w_{pi} &= \frac{nq^2}{e_0 me} \end{aligned} \tag{1}$$

The frequencies are therefore dependent upon plasma magnetic fields (B) and density (n). As will be shown in the Alfven wave discussion, the resulting wavelengths are also dependent on these parameters.

B. Alfven Waves

1. Propagation

The Alfven wave is defined by propagation in a magnetized plasma at frequencies below Ω_{ci}. At these relatively low frequencies, the ions and electrons move together, and their momentum also perturbs the ambient magnetic fields. This motion is described by the wave dispersion relation, which results from the simultaneous solution of the equations of motion and Maxwell's equations for both the electrons and ions. In the case of planetary plasmas, both electromagnetic motion and acoustic motions must be included, which results in three possible modes.

The full Alfven dispersion relation for a purely axial magnetic field is

$$D = \frac{(-B_{0z}{}^2 k_z{}^2 + \mu_0 \rho_0 \omega^2)(B_{0z}{}^2 c_s{}^2 k_z{}^2 (k_\perp{}^2 + k_z{}^2) - (k_\perp{}^2 + k_z{}^2)(B_{0z}{}^2 + c_s{}^2 \mu_0 \rho_0)\omega^2 + \mu_0 \rho_0 \omega^4)}{\mu_0{}^2 \rho_0{}^2 \omega^4 (-c_s{}^2 (k_\perp{}^2 + k_z{}^2) + \omega^2)} \tag{2};$$

the full dispersion for a three dimensional magnetic field is more complicated. Additionally, the effects of damping, either viscosity or resistivity, can be included in the dispersion derivation – this was done in this analysis, but is not a primary focus of the propagation analysis, as these parameters are not well known for astrophysical plasmas[13].

Alfven Modes

The full equation is sixth order, which yields three distinct modes that can occur in the Alfven frequency regime.

$$\begin{aligned} w &= k_z V_A = k\cos(q) V_A \quad (shear) \\ w &= k V_A \quad (compressional) \\ w^2 &= k^2 (V_A^2 + c_s^2) \quad (magnetoacoustic) \end{aligned} \tag{4}$$

where V_A is the Alfven speed ($\sqrt{B^2/m_0 r_0}$) and c_s is the sound speed ($c_s = \sqrt{qT/M_i}$). In these modes, the shear mode is strictly a parallel propagating wave (**k**=k_z), whereas the compressional and acoustic modes are capable of propagating across the magnetic field ($\mathbf{k} = \sqrt{k_z^2 + k_\wedge^2}$). This introduces the potential for some directionality in the propulsion system.

The shear mode is a purely parallel mode, representing a pure transverse wave. The compressional and magnetoacoustic modes allow for propagation perpendicular to the magnetic field, through compression of adjacent magnetic field lines. In these modes, the relative magnitudes of the parallel and perpendicular are free to vary, as long as the total wave number obeys the dispersion relations.

1. Parameters

Wave propagation therefore involves multiple parameters: ω, k_z, $k_\perp$, and the plasma characteristics B, ρ_0, and T, which vary with position in the planetary magnetosphere. The dispersion equation can yield solutions in terms of wave numbers k_z and $k_\perp$, as a function of the local plasma mass density (ρ_0) and magnetic fields and applied frequency. The dispersion equation also enables ray tracing analysis, through the coupled equations

$$\begin{aligned} \frac{\partial \vec{x}}{\partial t} &= -\frac{\partial D / \partial \vec{k}}{\partial D / \partial w} \\ \frac{\partial \vec{k}}{\partial t} &= \frac{\partial D / \partial \vec{x}}{\partial D / \partial w} \end{aligned} \tag{3}$$

By integrating these equations together, and allowing for the change in B and ρ with position throughout space, a wave's path through the magnetosphere can be traced. This tracing is essentially following the energy flow of the wave.

2. Antennas

Generating waves efficiently will require proper antenna dimensions and configuration to adequately match the antenna's electric and magnetic fields to those defined by the surrounding plasma's dispersion relation. The antenna radius and length, and axial spacing between antenna elements, all play a role in determining the wavelengths at which the antenna generates the highest fields. An example of the vacuum field spectra (in wavenumber space) is shown in for two antennae of differing length in . Both antennae are configured according to Figure 2, but with differing total length and spacings, as given in Table 1.

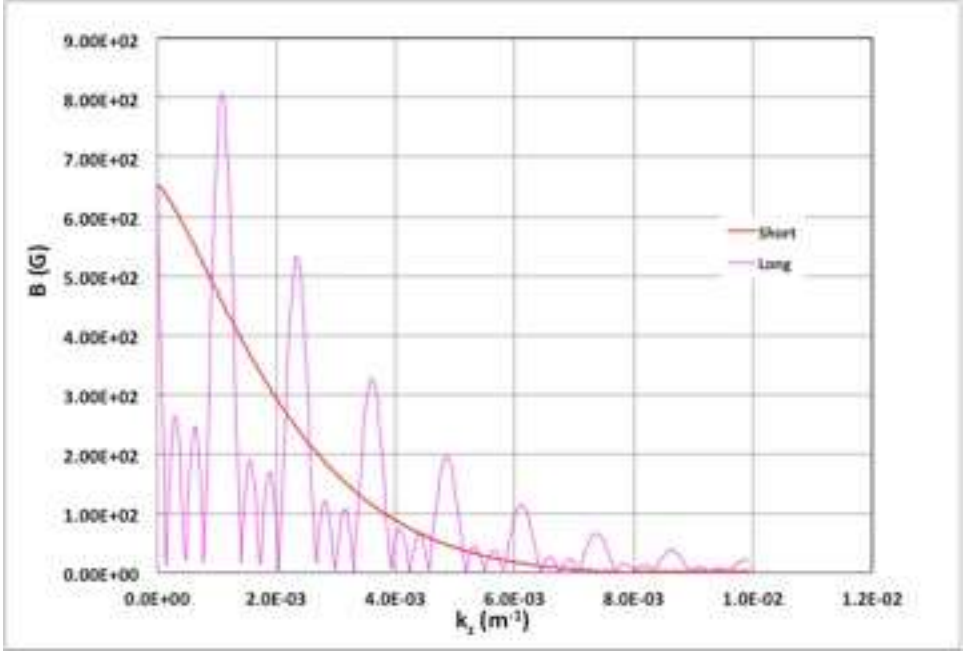

Figure 3. Sensitivity of antenna wavenumber to antenna length.

Additionally, two of the three Alfven modes propagate with a component perpendicular to the magnetic field, with a wavenumber $k_{\perp}$. In free space, the perpendicular wavelength can be somewhat arbitrary, or determined by gradients in the ambient fields. However, generation of waves by a cylindrical geometry, finite radius antenna also introduces constraints on the available $k_{\perp}$. In a purely cylindrical environment, perpendicular wavelength would be defined by both the antenna or plasma radius, and by the azimuthal wave number, m. Differing azimuthal modes ($\approx e^{im\emptyset}$) indicate the relative polarization of the wave, with m spanning the range of positive and negative integers and zero. This effect is seen in the coupling of the wave to a plasma, not a vacuum field, and will be shown in Section III.

Table 1. Test dimensions of antennae for spectrum in Figure 3.

Antenna	Length (km)	Separation (km)	Radius (m)
Short	3	1	500
Long	15	5	500

C. Planetary Magnetospheres

A planetary magnetosphere is generally a complex system arising from rotating planetary magnetic fields, plasma captured from from interplanetary space and the solar

wind, and the interaction of the magnetic field with the solar wind and solar magnetic fields. Typically, a magnetospheric model is used to interpret localized experimental data from spacecraft passing through the system, or to predict future activity in the magnetosphere – i.e. "space weather." These types of models deal with asymmetry in the magnetic field due to solar wind pressure, current sheets to allow separation of the planetary and interplanetary magnetic fields, and rotation of the planet. This level of detail is not needed at this stage in the investigation of plasma wave propulsion, as the focus is on the general feasibility of the concept.

1. Magnetospheric Models

For this assessment Jupiter's and Earths magnetic fields were modeled as axisymmetric dipole fields, with an accompanying radial magnetic field model. Models were taken from the literature, neglecting the more detailed aspects such as plasma tilt with respect to the solar wind, rotation, and the trailing current sheet for reconnection.

Jupiter

Jupiter has been examined extensively due to the large amount of spacecraft data obtained[14,15,16]. One result of some of these investigations was the observance of Alfven waves in the Jovian magnetosphere between 10 and 25 Jupiter radii (Rj)[17]. Alfven waves were also observed near the Io torus, a high density region surrounding Io's orbit and created by the escapes of particles from Io's active surface[18,19]. It was these results that lead to the concept considered here. Additionally, there have been measurements of Alfven waves in the vicinity of the Jovian plasma sheet; however, this was too localized a region to allow robust travel in a planet's orbit.

Instead, a simple dipole field was used to look at the potential performance and scaling of the concept throughout all of the Jovian magnetosphere.[20] The calculated vector field and magnitudes of the total B field are shown in Figure 4. The nature of the dipole field is that it is axisymmetric; therefore, calculating the field as $\{\vec{B_x}(x, z), \vec{B_z}(x, z)\}$ is adequate to describe propagation throughout the magnetic field.

Jupiter's density is modeled as a purely radial varying field, $\rho(x, z)$[21]. Most data include the effects of Io's plasma torus, due to the astrophysical interest in this feature. This will provide an interesting option and test of the wave launching, as most magnetospheres (such as Earth's) have a monotonically decreasing density field. The Jupiter density function is shown in Figure 5. The effect of the Io plasma torus on wave characteristics is shown in Figure 6, through the variation in Alfven speed throughout the Jovian magnetosphere.

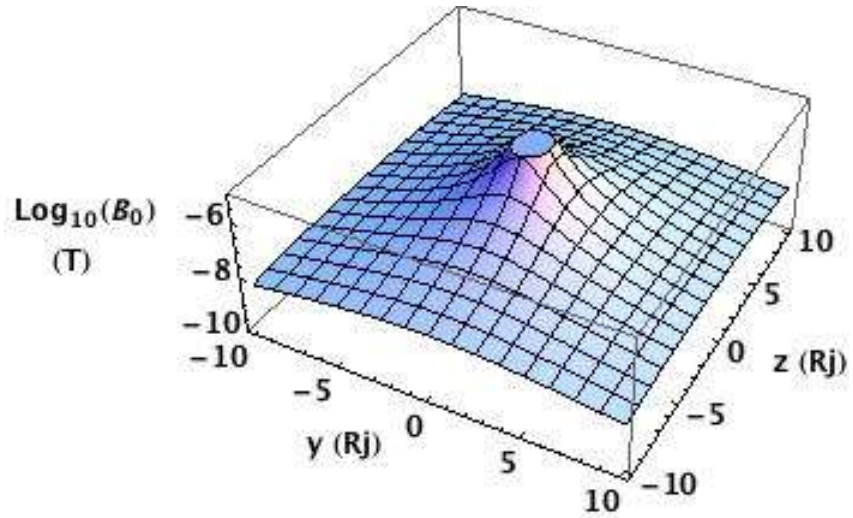

Figure 4. Jupiter dipole field profile in T.

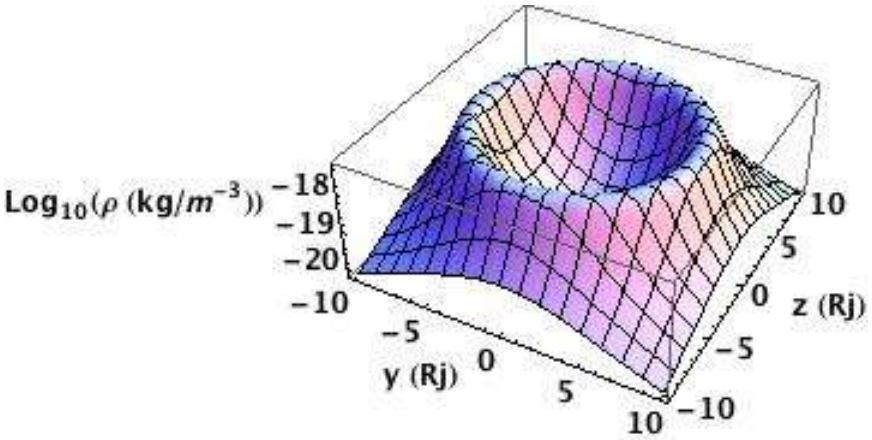

Figure 5. Jupiter plasma density profile including Io torus.

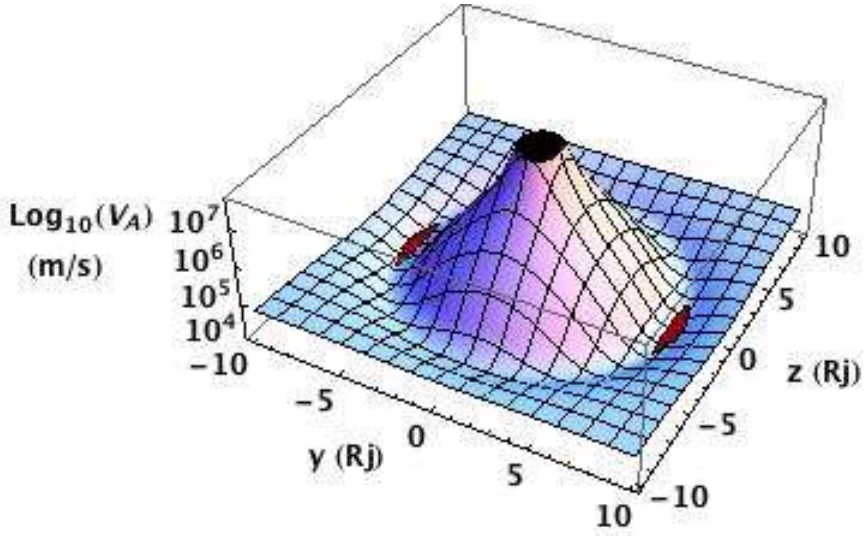

Figure 6. Alfven wave speed variation with position in Jupiter's magnetosphere.

Earth

Earth's density is also considered as an axisymmetric distribution[22]. Earth's magnetic and plasma environment are shown in Figure 7 through Figure 9. There is a slight increase in plasma density at outer radii, but this is not as pronounced as that observed at Jupiter. This provides an interesting contrast in the wave propagation conditions between the planets. Also, while the range of Alfven speeds overlap between the two planets, Jupiter's environment also includes regions of slower speed compared to Earth.

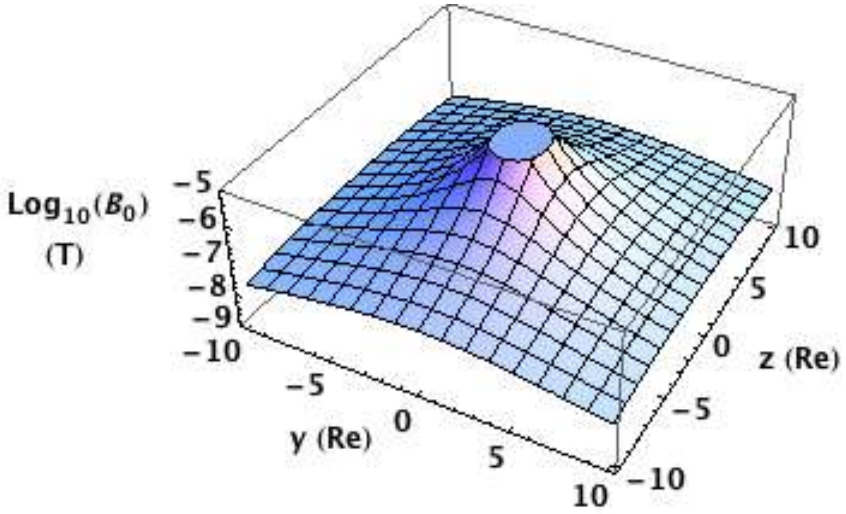

Figure 7. Earth magnetic field variation .

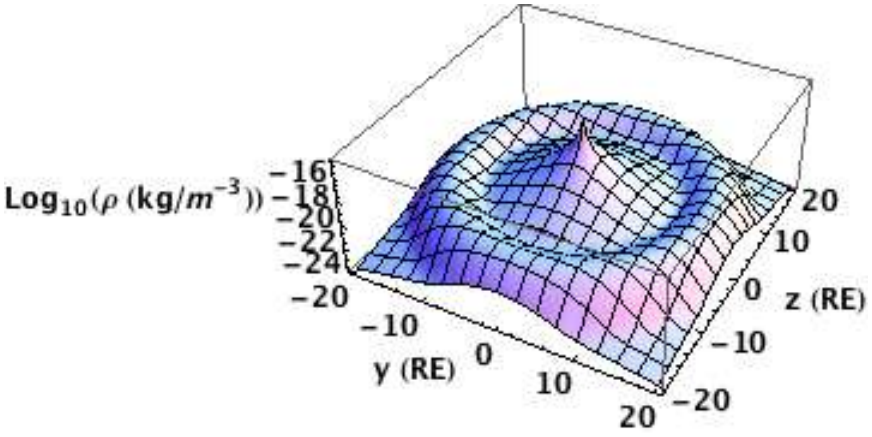

Figure 8. Earths' plasma density distribution through the magnetosphere.

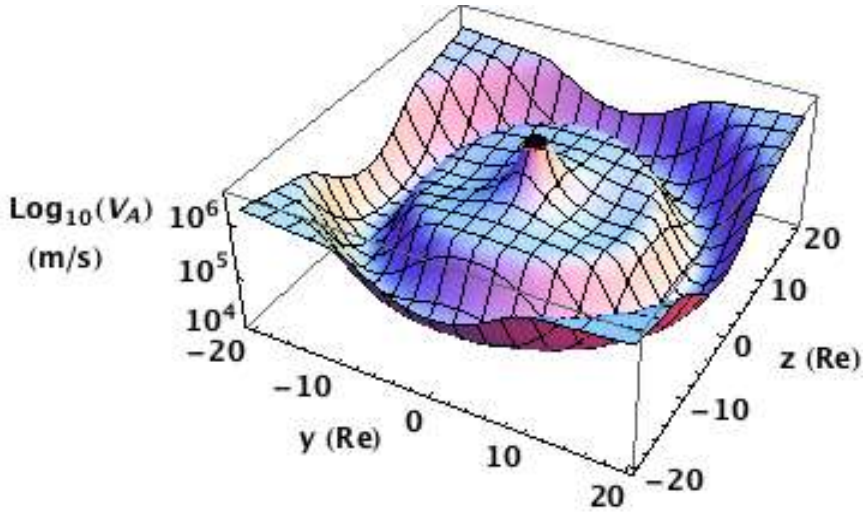

Figure 9. Alven wave speed values in Earth's magnetosphere.

III.Results

A. Ray Tracing/Propagation in Relevant Environments

1. Modes

In both Jupiter and Earth magnetospheres, all three modes are considered at each point in the test matrix (Figure 12). For the two modes with arbitrary parallel and perpendicular combinations, an arbitrary perpendicular wave number was selected by setting it to be 100 times the value of the parallel number. This was done in recognition of the fact that the total wave numbers for the conditions around the planets are small (10^{-5} – 10^{-7} m^{-1}), indicating large wavelengths that would make antenna scales quite large. The perpendicular dimension, which would be related to antenna diameter, was chosen to be the smaller of the two dimensions, to make antenna construction more feasible. For each initial condition, the same ray tracing dispersion relation was used, including all the possible modes. This allows for a given ray to convert from one mode to another if required by the ambient conditions.

As a representative value, a frequency of 0.2 the local ion cyclotron frequency at each point in the matrix was used. This frequency was kept a constant through the ray tracing, with the wavelengths changing with position. Changing this frequency would change the available wavelength space, but for the initial feasibility assessment, the frequency was kept constant. Frequencies are quite low, at the level of Hz, for much of the magnetospheric environment.[23]

2. Initial conditions

The ranges of wave numbers for the fixed frequency described previously are shown in Figure 10 and Figure 11 for the Jupiter and Earth systems, respectively. These values represent antenna scale lengths on the order of 10 - 1000's of meters, depending on the mode considered. For an initial look at the feasibility of propagating human-generated Alfven waves in the magnetosphere, these values of k_z and $k_\perp$ were used at each point in the matrix to examine the paths of the waves. Viewing the local magnetic field as the local z direction, $k_\perp$ is then a vector in a combination of the x and y directions, { k_x, k_y, 0).

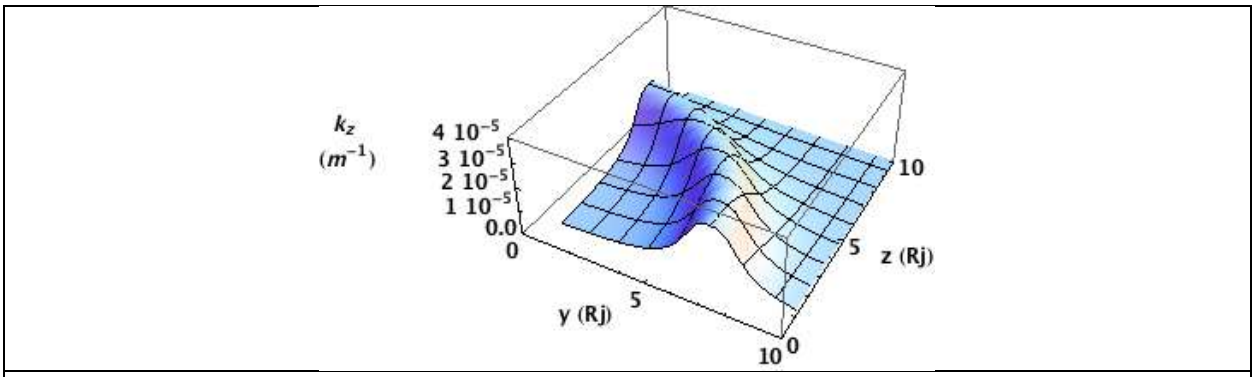

Shear

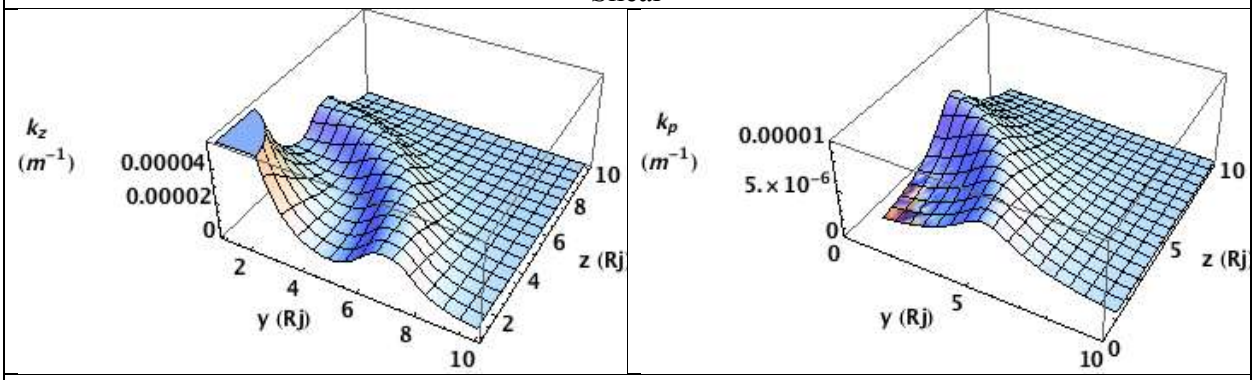

Magnetoacoustic

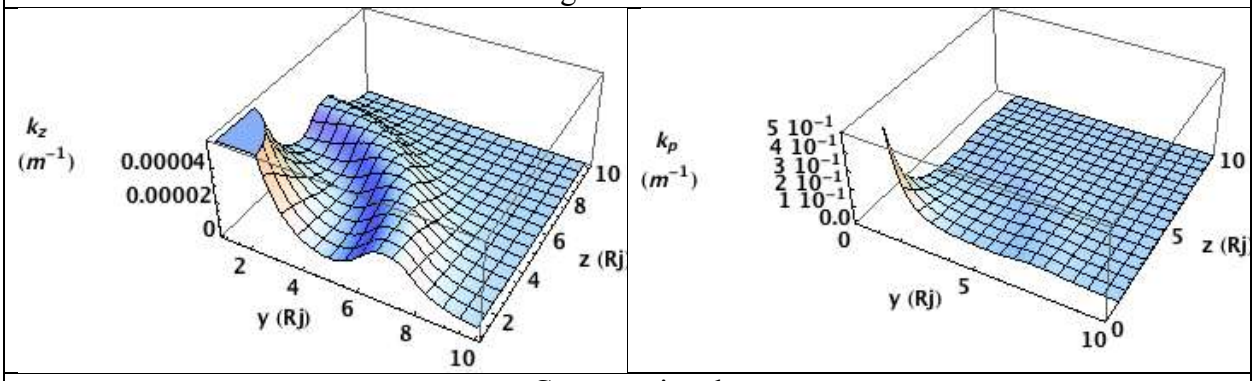

Compressional

Parallel wave numbers (k_z)	Perpendicular wave numbers ($k_\perp$)

Figure 10.Alfven wave numbers for each mode throughout Jupiter's magnetosphere.

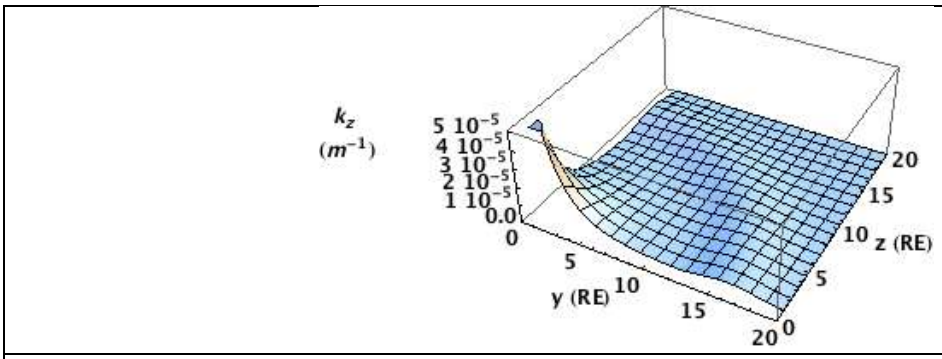

Shear

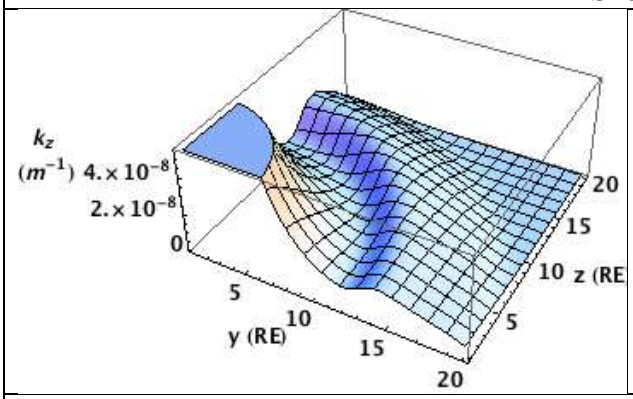

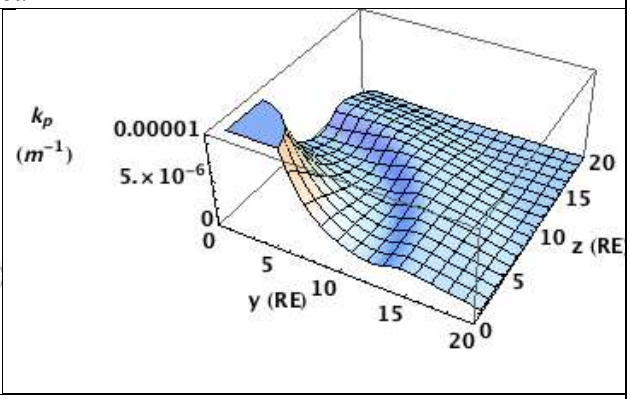

Magnetoacoustic

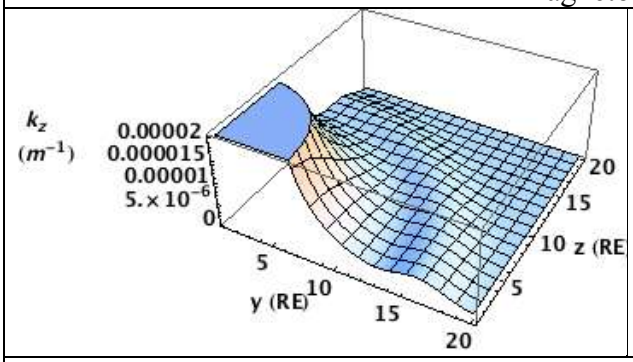

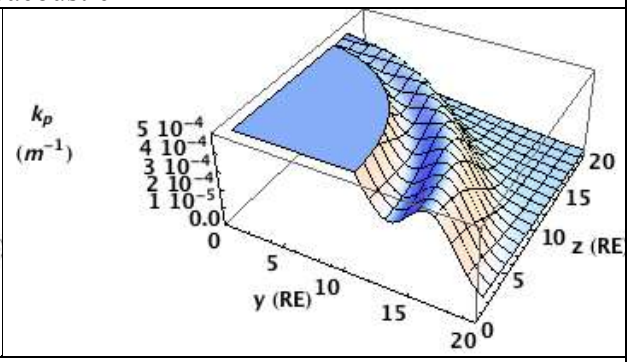

Compressional

Parallel wave numbers (k_z)	Perpendicular wave numbers ($k_\perp$)

Figure 11.Alfven wave numbers for each mode throughout Earth's magnetosphere.

3. Wave Launching in Relevant Environments

Ray tracing was performed using the Mathematica program, with wave launching starting parallel to the local magnetic field, using the locally matched wavenumbers calculated for each mode. All three modes were launched at each location, in that the differing k_z and $k_\perp$ for each mode was used as a separate initial condition. Thus, for each spatial location, three different types of Alfven wave were launched. The positions selected for this examination are shown in Figure 12, in terms of coordinates normalized by the planetary radius.

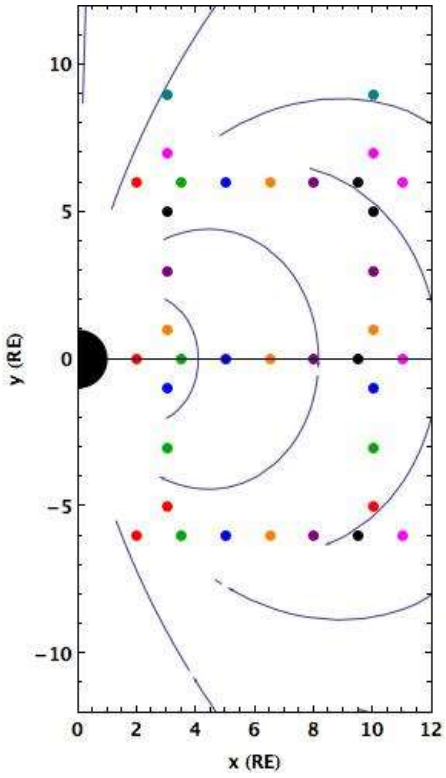

Figure 12. Test points for initial launch of Alfven waves in representative magnetosphere.

As the waves are traced through the magnetosphere, several results are possible along the trajectory: the wave propagates, the wave reaches a resonance condition (energy is absorbed, and wavenumber goes to infinity) and stops, or the wave reaches a cutoff (becomes evanescent) and is reflected. Numerically, the resonance condition introduces numerical errors which can result in the solution diverging. Reflection is, in general, followed by the integration. Propagation, damping, and/or absorption away from the launching point are all acceptable results, which allow for the wave to impart momentum at the launching site. The possibility exists, however, in a closed magnetic field system, for waves to return to their origin, which would in turn result in standing waves and no propulsive effect. It is this question that the ray tracing must answer.

Ray paths were integrated in time from the initial (x, y, z, k_x, k_y, k_z) for each position and mode. In the tracings shown herein, the perpendicular wave number was set to be in the plane of the B field: that is, if the dipole field is shown in {y, z} plane, $k_\perp$ is also in the {y, z} plane. This allows the ray paths to be shown in one plane. By setting $k_\perp$ in the x direction, the perpendicular modes must be shown in three dimensions. One example of these paths will also be shown, but is harder to visualize.

The calculated paths were integrated over 100's of wave periods, to allow for full assessment of the rays' ultimate destinations and behavior. In some instances, the rays would reach a resonance or region of strong gradients in the dipole field, resulting in a sudden jump in the ray speed and an abrupt straight line trajectory. This can be viewed as either a numerical response to a resonance condition in the fundamental equations.

The ray tracing results are shown in two different ways: first, the ray paths from each row or column of points considered in the magnetospheres, showing each of the three modes' paths launching at each point. The second way of showing the rays is to show the paths of each mode from all of the positions. Some general conclusions can be drawn as to the feasibility of the various modes and positions for propulsion, particularly in terms of the reflection potential of the various modes and positions.

Jupiter

Jupiter's case is shown in Figure 13 , showing all the modes launching from each row or column of points defined in Figure 12. The paralle modes are shown as solid lines, and the perpendicular modes are dashed or dotted lines. In certain regions, such as the Upper and Lower Horizontal at radii around 7 Rj, the wave paths do in fact appear to resonate around Jupiter, which would result in standing waves and no propulsive effect.

In order to more clearly determine the modes/initial conditions that yield the resonance condition, and to identify the propagation directions for those that could provide propulsion, the individual mode paths are plotted in Figure 14 for each of the sets of locations. In this way the compressional mode appears to be the mode that results in resonances, where the other modes propagate indefinitely or reach a nonlinearity in the integration. For the regimes where the resonance occurs, the initial conditions and system parameters would have to be altered, either in terms of frequency or wave spectrum, in order to allow propulsion.

Earth

Similar calculations for the Earth's magnetosphere are shown in Figure 15 and Figure 16. Resonances occur at several locations in this trial calculation (as is seen in Figure 16), primarily occurring in the magnetoacoustic and compressional modes. Although it appears that the resonances actually appear in channels that do not coincide with the originating launch points; in this case the propulsive effect would be maintained. For the initial conditions used, this channel occurs in a radial region between ~12 and 15 Earth radii. This calculation echoes the naturally occurring cavity modes postulated and/or observed in terrestrial or Jovian magnetospheres, driven by the solar wind[23,24]. The outermost points in the test matrix, closest to the radial resonance zone, would be the most susceptible to a resonance (non-propulsive) condition, and the frequency or wavelength would have to be adjusted for transit in this regime.

As noted previously, the wave propagation can also be calculated using an out of plane $k_{\perp}$ values. An example of this type of ray path, which must be viewed in three dimensions, is shown to illustrate this form of the waves. This result is shown as ray paths in the xy plane in Figure 17, after the yz plane wave paths, for Jupiter, in three dimensional form. Some similar resonance behavior is seen in these graphs, but drawing conclusions on the regions and types of resonant paths is harder in that geometry, and beyond the scope of this report.

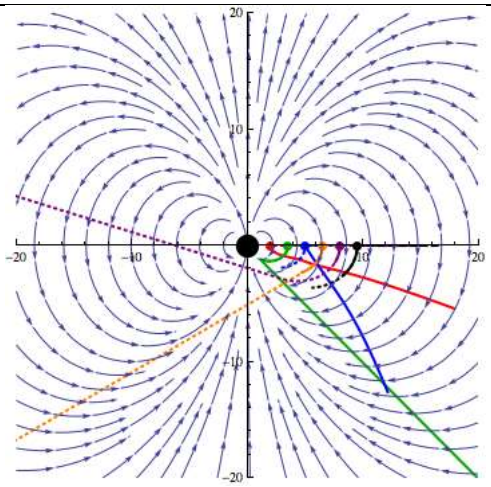

Equator

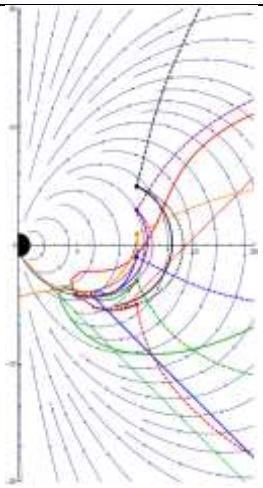

Outer Vertical

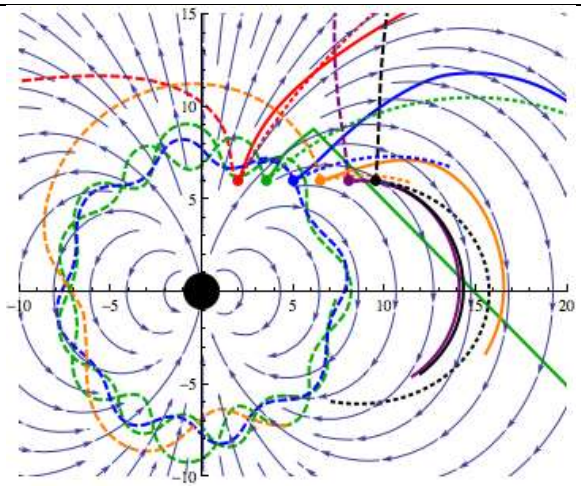

Upper Horizontal

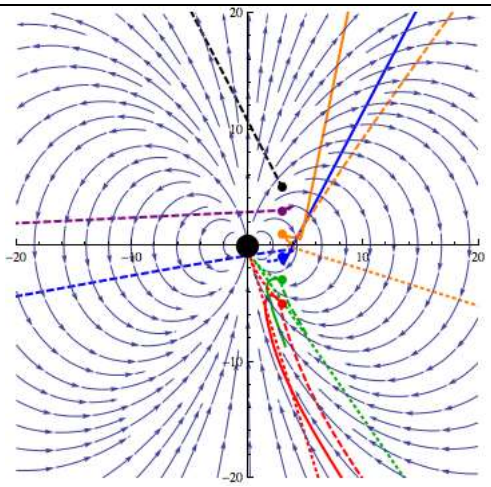

Inner Vertical

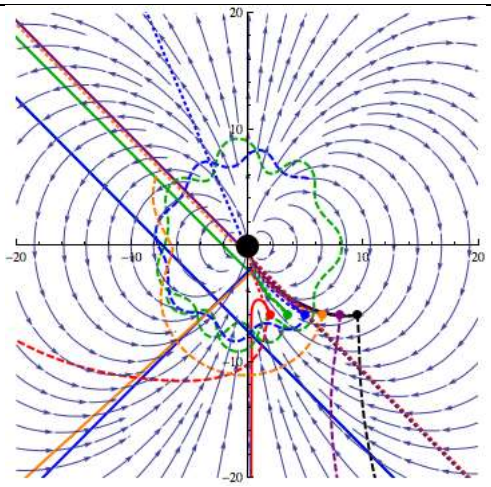

Lower Horizontal

Figure 13. Jupiter wave propagation from various positions in the magnetosphere.

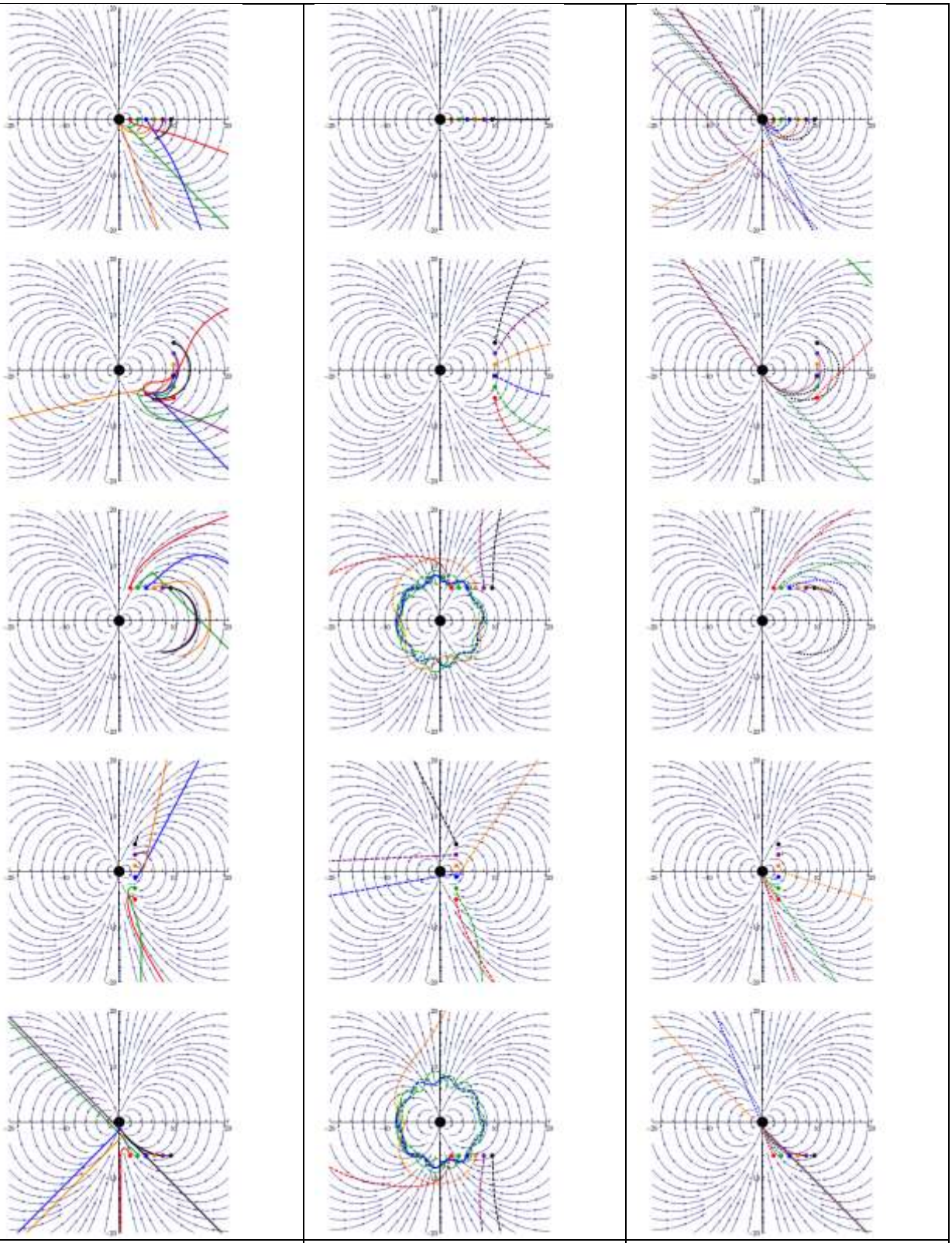

Magnetoacoustic	Compression	Shear

Figure 14. Paths of the three Alfven modes through Jupiter's magnetosphere.

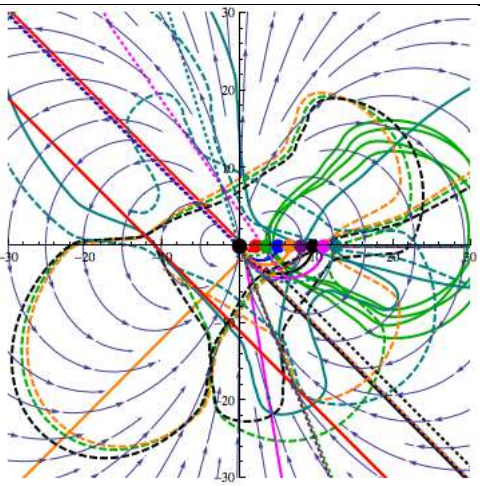

Equator

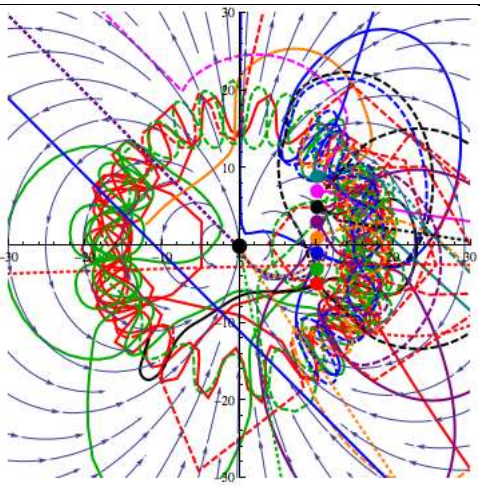

Outer Vertical

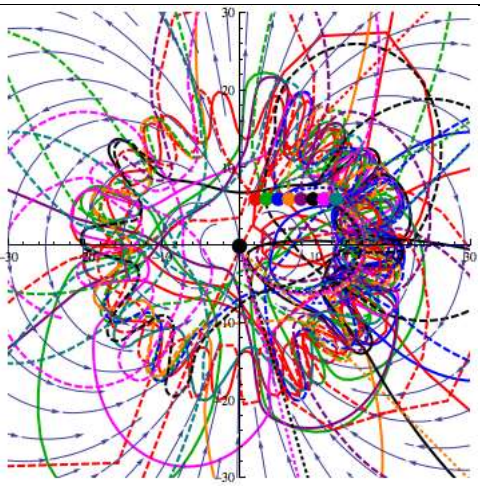

Upper Horizontal

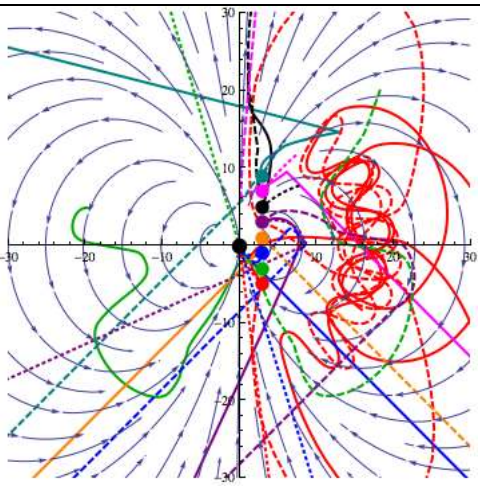

Inner Vertical

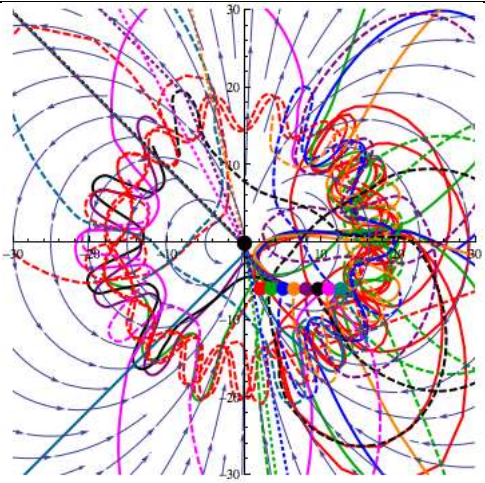

Lower Horizontal

Figure 15. Earth wave propagation from various positions in the magnetosphere.

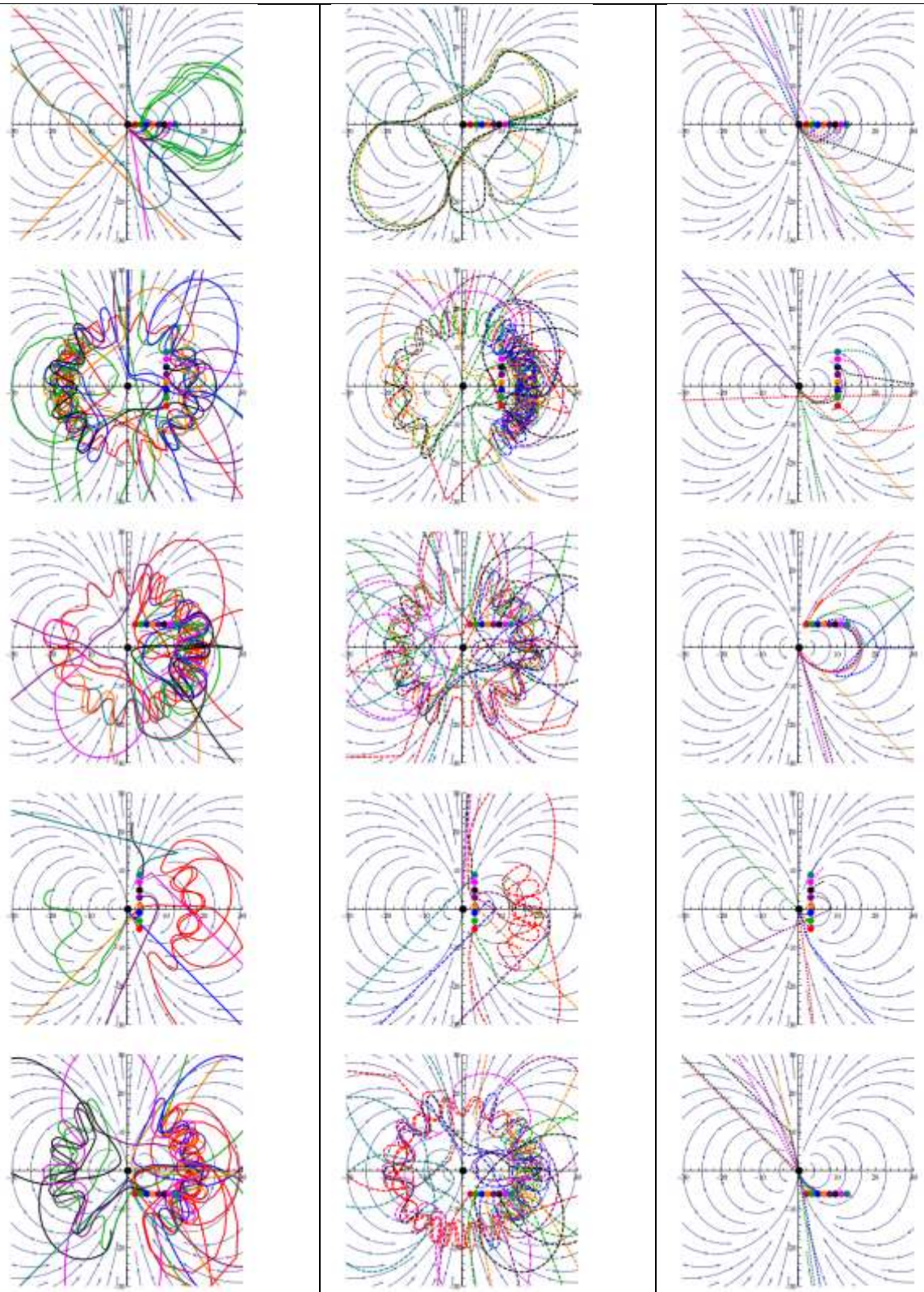

Magnetoacoustic	Compression	Shear

Figure 16. Paths of the three Alfven modes through Earth's magnetosphere.

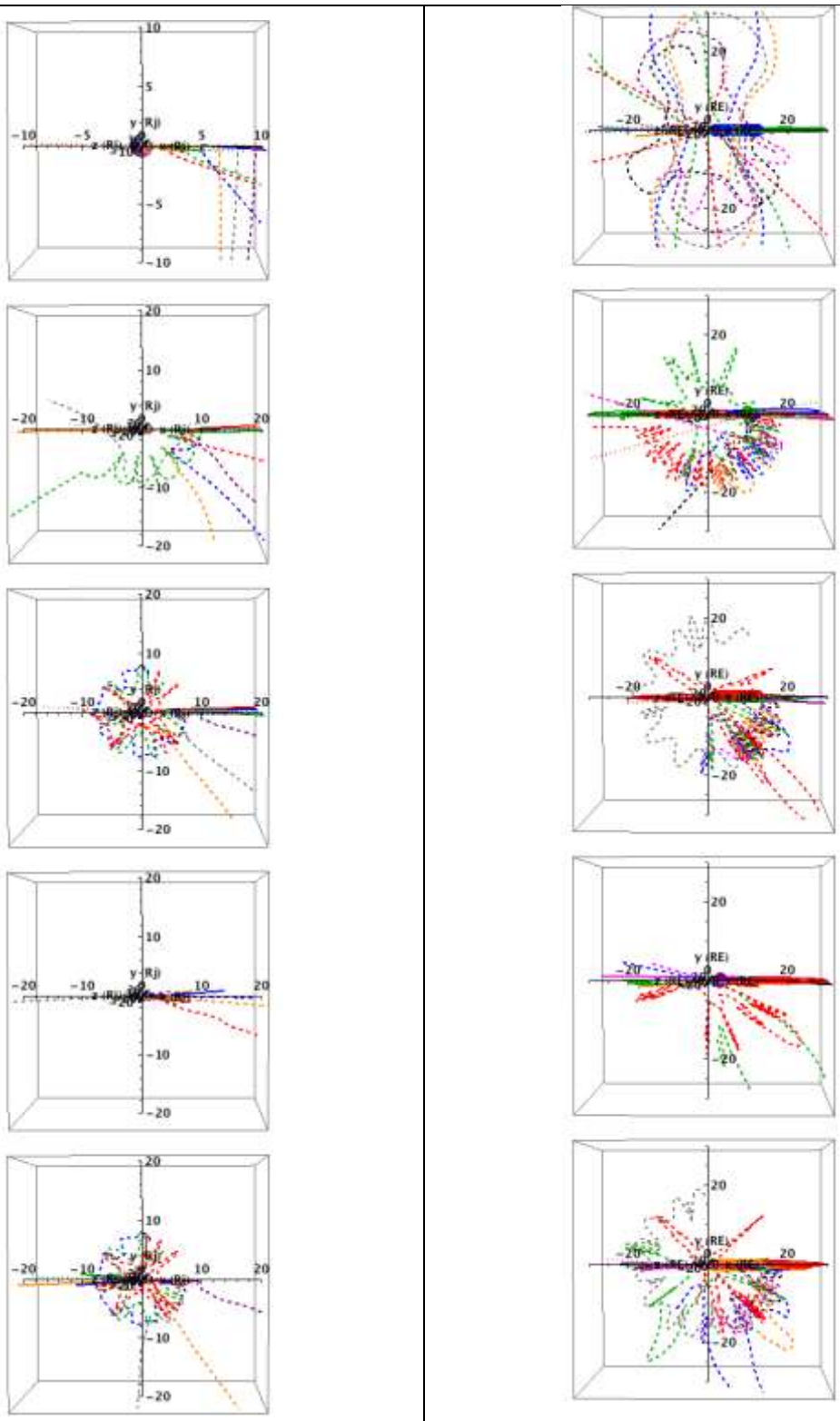

Jupiter	Earth

Figure 17. Wave propagation in x-y plane for $k_{\perp}$ in y direction.

B. Antenna Examples

The interaction with the antenna and plasma spectra was analyzed using the ANTENA code, which can calculate the wavelength spectrum of the antenna-plasma coupling in terms of loading or power delivered. The coupling and propagation of an actual antenna design to Alfven wave propagation was assessed at conditions taken from the Jupiter magnetosphere, at a radius of ~ XX Rj. These parameters are given in . The coupling of several antennae was assessed to estimate the effectiveness of the overall wave launching system as a propulsion system. Thrust was determined from the field strength of the waves leaving the antenna, integrated over the cross sectional area of the antenna. Coupling of the antenna was measured in terms of the resistive load on the antenna from the plasma – this, combined with the imposed antenna current, gave an estimate of the power required.

Table 2. Input plasma parameters For ANTENA modeling.

Parameter	
B_0 (T)	1.40×10^{-9}
n_i (m^{-3})	6.04×10^{7}
T_e (eV)	100.0

Some trades on antenna design were performed, which will not be described in detail. The 4-coil antenna design allows for flexibility in terms of coil separation, overall length, and the polarization of the waves. Trades in terms of phasing of the coils, both in terms of the relative phase of current from one coil to the next ($\pi/2$, $\pi/4$, $\pi/8$), and the direction of the rotation (positive or negative), were considered. At phasing of $-\pi/4$ was found to be most effective in terms of coupling to the plasma most effectively. Some trades of antenna length (see spectra discussion below) are described as examples of the design process involved.

1. Spectra

For a representative plasma environment, the ANTENA-calculated vacuum field sensitivity to axial separation/length, as well as to the relative phasing of the elements, are shown in Figure 18 and Figure 19. In Figure 18, spectra are shown for several different length antennae for a fixed azimuthal mode number. This result, with plasma present, can be compared to the example vacuum spectra shown in Figure 3. Note that while the general trends are the same, the relatively higher peaks of the long antenna compared to the short one in vacuum are not as pronounced in the presence of plasma, due to the plasmas inherent reaction to the fields based on densities and field strengths. The highest loading occurs at small wave numbers ($2\pi/\lambda_z$), which implies large antenna separations, up to 10^5 km. A discrete spectrum with narrow, specific loading peaks is obtained at the larger sizes; this is because the available wavelengths are narrower for a longer antenna. Shorter antennae appear to the plasma as spatial delta functions, which generate a broader spectrum.

In Figure 19, the change in loading for a fixed antenna length is shown for several m values. An m=0 mode is axisymmetric; the nonzero values denote fields which can rotate either right or left about the axis depending on the sign of m. The dominant wavenumber differs for each mode, and overall wave coupling could result from a combination of several azimuthal modes, rather than on single mode. In calculating antenna loading and wave fields for a short and long antenna, ANTENA includes up to 30 azimuthal modes in the calculations.

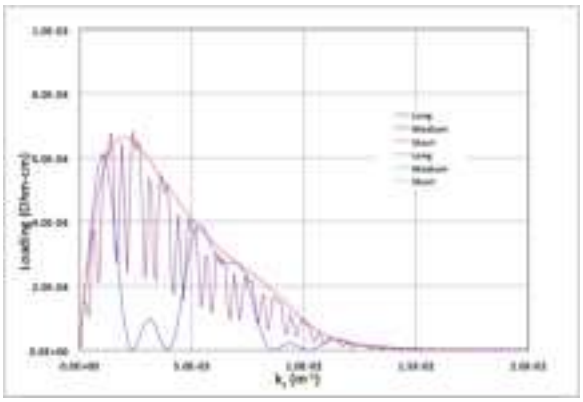

Figure 18. Plasma loading spectrum for a range of antenna lengths.

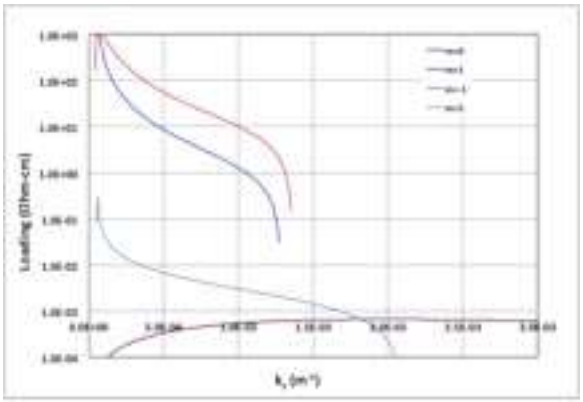

Figure 19. Plasma-antenna loading for various azimuthal mode numbers.

2. Fields

Wave fields for the short and long antenna configurations were calculated for multiple azimuthal numbers at a nominal antenna current of 10 kA. The current was chosen to generate magnetic fields in the plasma that were less than or comparable the ambient field, in order to maintain the linearity of the waves that is assumed in both the ray tracing and ANTENA analyses. The axial variation in wavefields was calculated at radii of 100 and 10000 m, to get an indication of the variation in radius. The wave fields shown are actually for the left polarized electric fields of the plasma, which takes in to account the azimuthal number and gives a clearer view of the wave propagation and the phase velocities.

The propagating fields for the short and long antenna options are shown in Figure 20 and Figure 21, respectively. Both show highly peaked fields near the antenna straps, with a lower level of energy propagating away from the source. The magnetic field oscillation is smaller relative to the mean than the electric field, but the electric field confirms a left polarized wave propagating away from the antenna. The wave magnitudes are comparable between the two options. The symmetry of waves in either direction is problematic; if the wave energy is the same in both directions, zero net thrust would result. To determine this balance, the wave magnetic pressure ($\partial B^2/(2\,\mu_0)$ at either edge of the antenna was integrated over the antenna aperture area at a distance of 2 x 10^5 m from each antenna edges, away from near field effects.

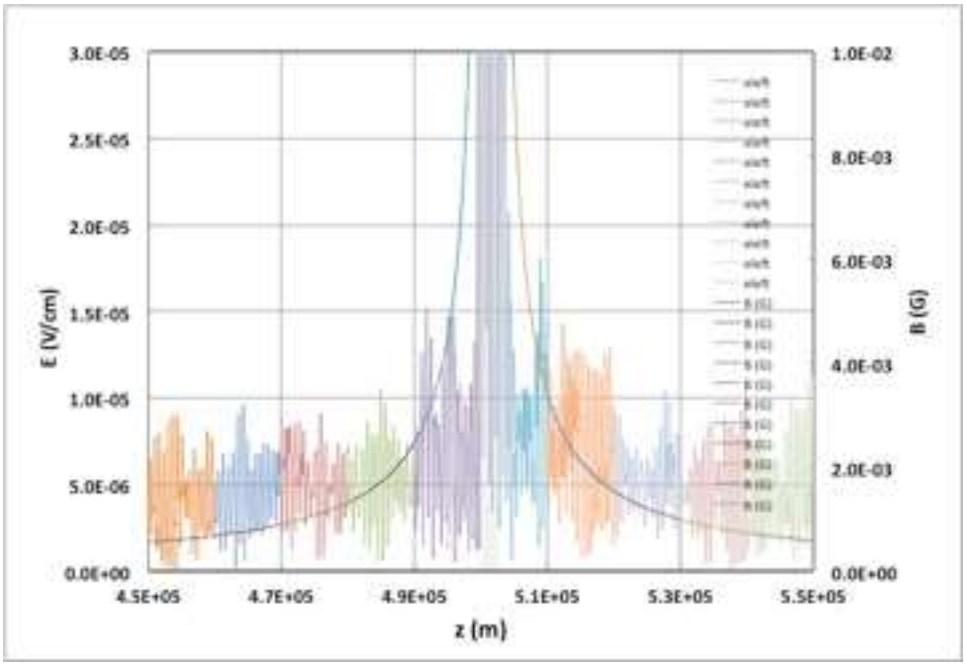

Figure 20. Short antenna wave electric and magnetic fields – antenna located at 5 -5.01 x 10^5 m.

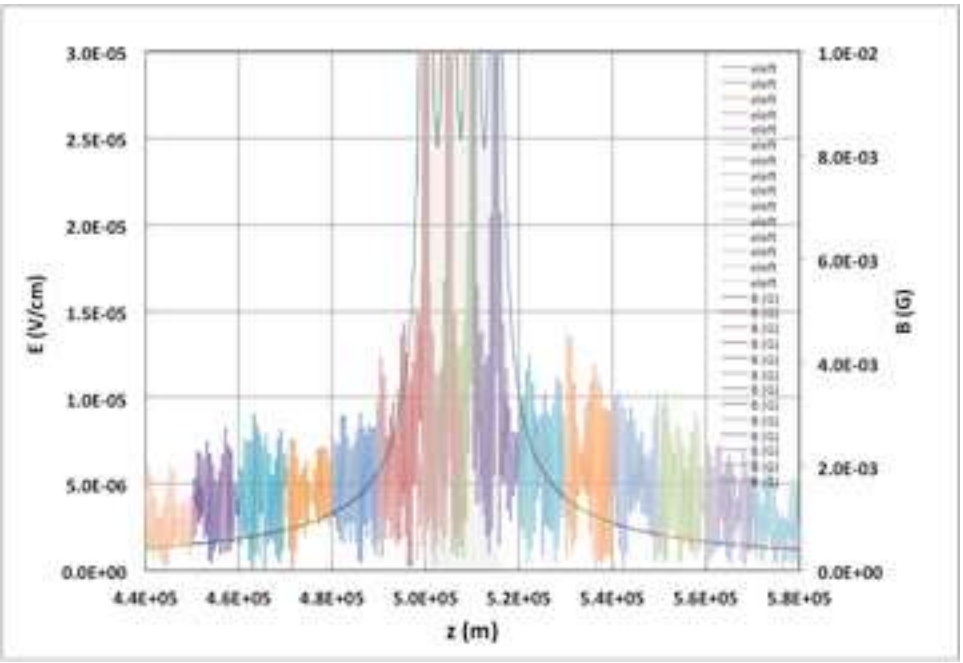

Figure 21. Long antenna wave electric and magnetic fields – antenna located at 5 -5.05 x 10^5 m.

Radial profiles for the long and short antenna at either edge are shown in Figure 22. Slight asymmetries are observed for both, with a stronger asymmetry in the short antenna case. The force at either edge of the antenna and the difference are shown in Table 3. This force is spread over a circular aperture of 500 m diameter, or ~2 x 10^5 m^2. The corresponding thrust densities are also

shown in the table. For comparison, the equivalent thrust density of the NEXT ion engine at full power (7.1 kWe) is 0.38 N/m^2. [25] Of course, these are first results estimates for this concept, and do not represent optimized per-formance. As further work/optimization is done on this concept, better field generation will be required to improve the acceleration potential of this type of system. Of course, also to be considered is the fact that the NEXT thruster requires propellant, with a finite specific impulse (I_{sp}) of 4200 s, whereas this lower thrust system requires only a power supply and the antenna itself.

Table 3. Forces at antenna apertures and net force.

	Forces (N)			
Antenna	**Left**	**Right**	**Net (➔ positive)**	**Thrust Density (N/m^2)**
Short	703	480	-223	1.1 x 10^{-3}
Long	399	402	2.53	1.3 x 10^{-5}

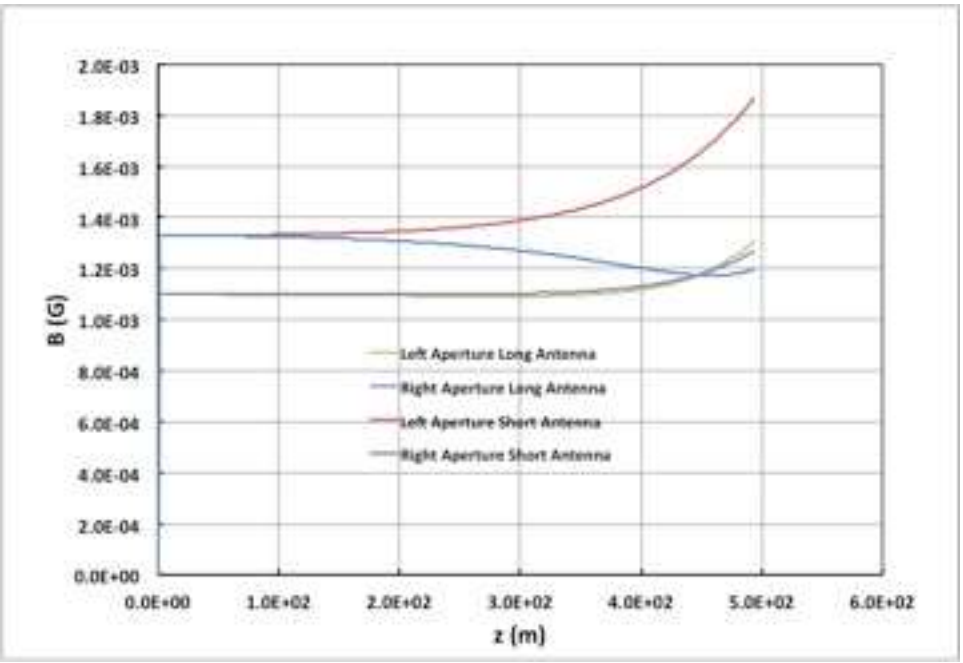

Figure 22. Radial magnetic field profiles for two antenna geometries.

3. Coupling/Power Deposition

ANTENA calculates the power absorbed by the plasma, and the impedance of the plasma to the antenna, in ohms. These values are shown in . For both antennae, a fixed current of 10^4 amperes was assumed. The power absorbed at the plasma edge, as well as the overall power provided to the antenna circuit, are calculated. As might be expected from a first estimate, the performance is very low. It should be noted that the calculations here do not include matching circuits usually required for any antenna circuit, which would allow better coupling to the overall system.

Taking the total antenna impedance as that seen by the circuit, the total input power to the (unmatched) circuit would be 1.3 GWe, of which very little (1.3 MWe) would be radiated to the plasma – the imaginary power would be deposited in the near field, which is not considered to be contributing to the radiation pressure in the far field.

Table 4. Antenna coupling and power requirements for 10 kA current.

	Power Absorbed (W)	Real Power (W)	Complex Power (W)	R (Ohm)	X (Ohm)	Z (Ohm)
Short	14.6	1.28×10^{6}	1.32×10^{9}	2.56×10^{-2}	26.4	26.4
Long	14.9	1.17×10^{6}	1.33×10^{9}	2.34×10^{-2}	26.4	26.4

C. System Performance

Several system aspects of this concept were assessed in this initial study with respect to fields generated and power requirements:

- Antenna phasing
- Antenna length
- Antenna polarization

The first configurations evaluated show that the concept is physically possible, in that waves can be generated from an antenna in a magnetosphere that provide a net radiation pressure for propulsion. However, the initial performace is poor based on the poor coupling of the antenna to the plasma. From this, the system performance challenges that need to be addressed by further work have been identified.

1. Design

The initial antenna dimensions and geometry prove to have poor coupling to the ambient plasma. This is due primarily to the large wavelengths required for wave propagation in contrast with the need for a relatively compact spacecraft/propulsion system. The first antennae considered are relatively simple, to evoke the sensitivities inherent in this approach. A primary limitation in the initial effort was the assumption of a small diameter (relative to wavelengths) antenna, which limited the coupling in the perpendicular directions. The short antenna system as analyzed would consist of 4 phased antenna straps in parallel, spaced 1 km apart and a total length of 3 km for the system. Ten kiloamperes of current were passed through the system, which would imply the need for superconductors to minimize resisitive losses in the straps.

2. Thrust and Power

Net thrust can be generated in this concept, but the first calculation showed a value of 223 N for the design described above. This arose from 14.6 W of absorbed power in the plasma, 1.3 MWe of radiated power, and 1.3 GWe of total power, due to the poor antenna coupling. As seen in Figure 20 and Figure 21, the near fields are more than 10 times the far fields, where the thrust was calculated.

IV. Conclusions

This initial analysis of the concept of propellantless propulsion using plasma waves launched in ambient plasma and magnetic fields examined

- Wave propagation in planetary magnetospheres
- Sensitivities to antenna phasing and scale

- Antenna coupling

Fundamental physics concerns of this study were identifying the necessary conditions and resulting behaviors for generating human-made Alfven waves in a planetary magnetosphere. Identifying the wavelengths and field strengths for successful waves was necessary for later design and assessment of antennae for a system assessment. Further, the potential for standing wave generation on a planetary scale, which has been observed in nature, had to be analyzed to show that it wave propagation would be possible without such standing waves, which prevent net thrust generation.

The engineering concern is the operation of antennae for a plasma environment, scale, and application never before considered. Because of the novelty, analysis techniques were adopted from some fusion applications, as well as some fundamental models developed for this specific concept. For initial scoping, a simple, flexible antenna configuration of 4 separate semicircular loops, located at $\pi/2$ from each other, was selected. Analysis identified phasings, polarities, and spacing trends that resulted in one design offering better coupling and field generation than the others.

Wave propagation modeling showed the potential for propagating several modes of the Alfven wave in much of the planetary magnetosphere from 2 – 20 radii. In some radially localized regions, modeling showed that standing waves could indeed arise under the conditions assumed, which would require some "throttling" of the system, probably in frequency, to avoid, either through changing the mode or the absorption of the wave. Both perpendicular and parallel modes appear to be possible to excite, from a fundamental existence analysis.

The actual design of antennae to successfully generate such waves is still unresolved. The full trade space in antenna design, which was beyond the scope of this initial study, incorporates

1. Length/diameter
2. Geometric arrangement of straps/coils
3. Phasing of coil current
4. Polarization of coils
5. Current magnitude

Some aspects of items 1, 3, and 4 were examined in this study for fixed geometry and current, and two representative designs were tested. The two considered showed that one, a "short" (3 km) 4 strap system 500m in diameter, with antennas in $\pi/4$ phasing was superior to a longer design, in that a greater net thrust was generated. However, both antenna designs suffered from poor coupling efficiencies. One likely reason is the relative small diameter of the antennae, which impairs coupling to longer perpendicular wavelength modes for the Alfven wave modes identified. Other possible reasons may be the need for a better geometry in terms of number of coils/straps and connections.

Future Work/Challenges

The clear challenge in determining the full potential of this concept for future missions lies in further optimization/understanding of the antenna-plasma portion. This will entail improving the tools for assessing the antenna in an astrophysical plasma, and increasing the number of design variables, as described above. Much of this could be continued using the codes used in this study; however, alternative or dedicated codes would be preferable. The ANTENA code suffers from its limitations as a terrestrial, bounded plasma code, and a more realistic approach for the future would

be to adapt astrophysical wave codes to incorporate detailed antenna designs. Most astrophysical codes are aimed at assessing naturally occurring phenomena. In the context of focusing on Alfven waves, MHD codes might be amenable to this adaptation.

Alternatively, two aspects of the antenna/plasma interaction were not addressed in this study: non-linear fields and alternative plasma waves. Non-linear fields would involve generating magnetic fields comparable to or greater than the ambient ones, producing pulses of plasma that could be accelerated away from the spacecraft. Such non-linearities would obviate the need for frequency and wavelength matching, but could have further dissipative mechanisms that impeded their efficiency. Alternate plasma waves, such as Whistler waves, which couple to electrons, introduce a higher frequency range and potentially smaller wavelengths. Because they operate on electrons rather than ions, the overall thrust levels might be lower than for Alfven waves.

---

[1] Oleson, S., "Electric Propulsion Technology Development for the Jupiter Icy Moon Orbiter Project," AIAA Paper 2004 3449, July 2004.

[2] Johnson, Les, Young, Roy M., and Montgomery, Edward E., "Recent Advances in Solar Sail Propulsion at NASA," IAC-06-C4.6.01, 57th International Astronautical Congress, Spain, Oct. 2006.

[3] Zubrin, R.M., and Andrews, D.G., "Magnetic Sails and Interplanetary Travel," AIAA-89-2441, July 1989.

[4] Winglee, R.M., Ziemba, T., Euripides, P., and Slough, J., "Magnetic Inflation Produced by the Mini-Magnetospheric Plasma Propulsion (M2P2) Prototype," Space Technology and Applications International Forum, Paper STAIF CP608, Feb. 2002.

[5] Cosmo, M.L., and Lorenzini, E.C., eds., Tethers in Space Handbook, 3rd edition, Dec. 1997.

[6] Frisbee, R., J. Prop. & Power, 19 (6) 1129 (2003).

[7] Kivelson, M. G., A*dvances in Space Research* 36 (2005) 2077–2089

[8] Zarka, P., A*dvances in Space Research* 33 (2004) 2045–2060.

[9] Wukitch, S., *et al*., Phys. Rev. Lett. 77, 294 (1996).

[10] Srivastava, A. K., and B. N. Dwivedi, J. Astrophys. Astr. (2007) 28, 1–7.

[11] Stix, T., Waves in Plasmas. American Inst. Of Physics, NY, 1992.

[12] McVey, B. "ANTENA," Technical Report: PFC/RP-84-12, MIT Plasma Fusion Center, 1984.

[13] Khodachenko, M.L., T.D. Arber, A. Hanslmeier, H.O. Rucker, "Comparative Analysis Of Collisional And Viscous Damping Of Mhd Waves In The Partially Ionized Solar Plasmas," Hvar Obs. Bull. 23 (2004) 1, 1–14.

[14] Zarka, P., "Radio and plasma waves at the outer planets," Advances in Space Research 33 (2004) 2045–2060.

[15] Bagenal, F., "The magnetosphere of Jupiter: Coupling the equator to the poles," Journal of Atmospheric and Solar-Terrestrial Physics 69 (2007) 387–402.

[16] Belenkaya, E.S., "The Jovian magnetospheric magnetic and electric fields: effects of the interplanetary magnetic field" Planetary and Space Science 52 (2004) 499–511.

[17] Khurana, K. K., and M. G. Kivelson, "Ultralow Frequency MHD Waves in Jupiter's Middle Magnetosphere,' Journal Of Geophysical Research, Vol. 94, No. A5, pp. 5241-5254, MAY 1, 1989.

[18] C. T. Russell, D. E. Huddleston, K. K. Khurana, and M. G. Kivelson, "Waves And Fluctuations In The Jovian Magnetosphere," Adv. Space Res. Vol. 26, No. 10. pp. 1489-1498, (2000).

[19] Wright, A. N., "The Interaction Of Io's Alfven Waves With The Jovian Magnetosphere," Journal of Geophysical Research, Vol. 92, No. A9, Pages 9963-9970, September 1, 1987.

[20] Mahjouri, M. S., "Simulation of Charged Particle Motion in Jupiter's Magnetosphere," *Acta Phys.* Pol. A 92 Supplement, S-21 (1997)

[21] Khurana, K.K.; Kivelson, M.G. et al. (2004). "The configuration of Jupiter's magnetosphere". In Bagenal, F.; Dowling, T.E.; McKinnon, W.B. (PDF). Jupiter: The Planet, Satellites and Magnetosphere. Cambridge University Press. ISBN 0-521-81808-7.

[22] Russell, C. T., Khurana, K.K., Arridge, C. S., and Dougherty, M. K., "The magnetospheres of Jupiter and Saturn and Their Lessons for the Earth," Advances in Space Research 41 (2008) 1310-1318.

[23] Kivelson, M., "ULF Waves from the Ionosphere to the Outer Planets", UCLA Institute of Geophysics and Planetary Physics Publication Number #6264.

[24] Uberoi, C., "Alfven Waves in Magnetospheric Plasma: Micropulsations and Particle Acceleration," Physica Scripta Vol. T60, 20-31, 1995.

[25] Herman, D. A., G. C. Soulas, and M. J. Patterson, "NEXT Long-Duration Test after 11,570 h and 237 kg of Xenon Processed," IEPC-2007-033, *Presented at the 30th International Electric Propulsion Conference, Florence, Italy September 17-20, 2007*.